JOURNAL OF APPLIED ELECTROCHEMISTRY 22 (1992) 293–300

# Influence of the partial pressure of oxygen on the redox chemistry of multivalent elements in molten sodium tetraborate

P. CLAES, Z. BACANAMWO, J. GLIBERT

*Catholic University of Louvain, Department of Chemistry, CHAN, B–1348 Louvain-la-Neuve, Belgium*

Received 7 June 1990; revised 10 June 1991

Voltammetric determinations based on current measurements have been developed in order to allow an *in situ* evaluation of the redox ratios of multivalent elements in molten sodium tetraborate. The same technique has been used to study the influence of the partial pressure of oxygen in the gaseous atmosphere on the redox properties of sodium tetraborate melts. Experiments were carried out at 1273 K in solutions of chromium with oxidation states VI and III and of antimony with oxidation states V and III; the $P_{O_2}$ values ranged from $5 \times 10^{-5}$ atm to 1 atm. Log [Ox]/[Red] plotted against log $P_{O_2}$ shows linear relationships with slopes of 0.72 and 0.54 in the case of chromium and antimony solutions, respectively. These values lie close to the theoretical values of 0.75 and 0.50, respectively, which are deduced assuming conditions of equilibrium between oxygen and the solute. In agreement with these results, voltammetric and potentiometric determinations confirm Nernstian behaviour of the oxygen-oxide redox system.

## 1. Introduction

There are several applications which require that the multivalent elements dissolved in glass melts are directly evaluated in the melt itself; there has been a growing interest in the use of electrochemical techniques for this purpose. It is particularly useful to develop techniques which provide peak shaped signals rather than waves since the width of the electrochemical signals is in proportion to the absolute temperature. In the case of borates and silicates the signals extend over a large potential range. Differential pulse voltammetry and square wave voltammetry have been suggested and a quantitative *in situ* determination of cobalt [1] and iron [2, 3] in molten silicates has been achieved with these techniques.

The oxidation state of a glass melt, which is characterized by the ratio $R$, between the concentrations of the oxidized and reduced forms of a multivalent element, strongly influences the main properties of the final product. Until recently, this concentration ratio has usually been measured by instrumental or chemical analysis after quenching of the sample. Russel *et al.* [4] have shown that the measured values are correct evaluations of the ratios before quenching if only one multivalent element is dissolved in the melt and if its concentration is considerably larger than the physically dissolved oxygen concentration (e.g. 0.2 mol % in the case of $Fe_2O_3$). Chemical anaylsis of samples which had been equilibrated in various partial pressures of oxygen before quenching has led to the conclusion that the ratio $R$ relates to the ratio of the oxygen–oxide redox system [5].

The ratio $R$ may also be evaluated on the basis of the characteristic potentials of voltammograms of solutions containing the oxidized and reduced forms of multivalent elements [2, 6]. Such determinations are possible when no reference electrode is available. Indeed, the standard potential of a redox system and the equilibrium potential correspond, or are straightforwardly related respectively to, the half wave or peak potential and to the intersection of the mixed wave and the potential axis. The $R$ ratio is then obtained from the Nernst equation in which the two potential values, measured against an arbitrary potential, have been introduced. Accurate and reproducible potential data are needed. If, for instance, the redox reaction involves an exchange of two electrons, the difference between the equilibrium potentials amounts to only 11 mV at 1000° C in conditions when the $R$ ratios are 0.9 and 1.1, respectively. The random errors, which are expected in potential measurements in oxide melts at high temperature, have often been seen to reach a comparable amount. Moreover, rather large ohmic drops are caused by the high current densities which cannot be avoided in molten borates and silicates and, at the high temperatures needed for these investigations, residual currents are so large that electrochemical determinations can only be carried out where there are high solute concentrations.

## 2. Experimental details

### 2.1. *Apparatus*

The platinum crucible (1) (6 cm dia. and 7 cm high) containing the melt, was placed in a vertical compact alumina container (2) with an air-tight aluminum

0021-891X/92  

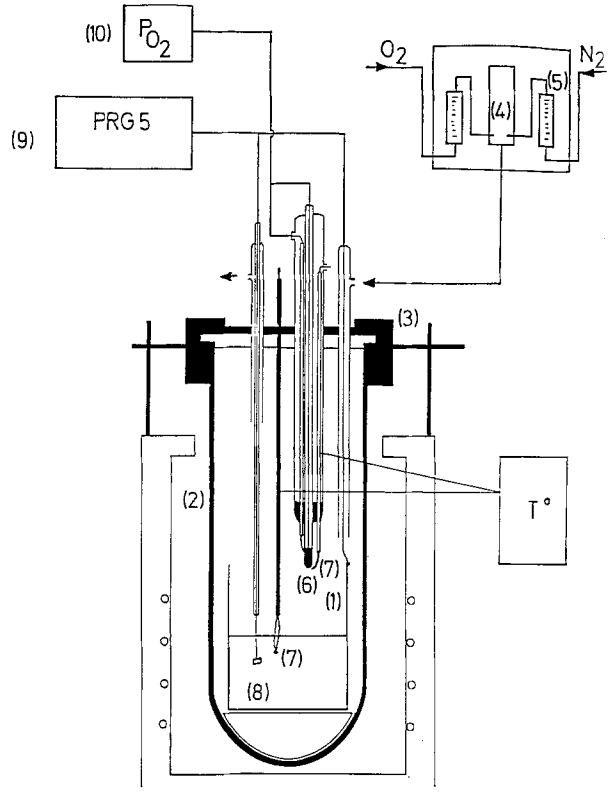


Fig. 1. Experimental device.

cover (3). This cover was cooled by means of a water jacket and fitted with "swage-lock" joints which allowed alumina tubes to be adjusted to chosen levels. These tubes acted as guides for the electrodes and the thermocouple and as the gas inlets and outlets. (Figure 1)

The power supply of the furnace was controlled by a NA3923 Honeywell regulator which in turn was monitored by a Pt–Pt 10% Rh thermocouple placed close to the alumina cell.

The partial pressure of oxygen ($P_{O_2}$) in the gas that flows through the alumina container was adjusted from $5 \times 10^{-5}$ to 0.76 atm by mixing air or oxygen with nitrogen in a buffer volume (4). The respective gas flows were regulated by means of precision valves and measured with calibrated flowmeters (5). The lowest oxygen partial pressure, $5 \times 10^{-5}$ atm, corresponds to the oxygen content in the nitrogen gas used.

$P_{O_2}$ was monitored, just above the melt, by means of a zirconia sensor (6). The reference gas inside the electrode was dry air. The potential difference ($\Delta E$) across the zirconia membrane is, according to Equation 1, related to the partial pressures of oxygen in the gas flowing inside ($(P_{O_2})$air) and outside ($(P_{O_2})$cell) the zirconia tubing.

$$\Delta E = \frac{RT}{4F} \ln \frac{(P_{O_2})\text{air}}{(P_{O_2})\text{cell}} \qquad (1)$$

A calibration plot of the zirconia electrode at 1273 K is shown in Fig. 2. The graph yields an experimental value of $RT/4F$ equal to $-27.0$ mV compared with the theoretical value of $-27.4$ mV. Fluctuations do not exceed $\pm 3$ mV and the gas flow has no influence on the potential differences at equilibrium.

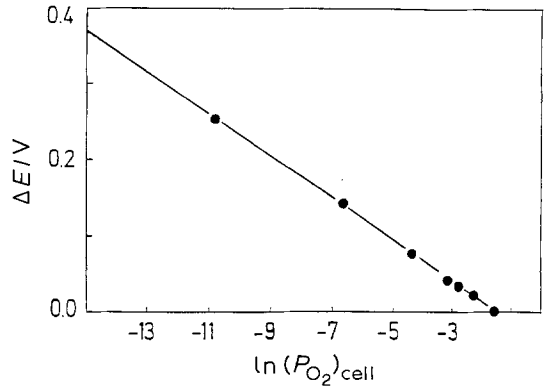


Fig. 2. Calibration plot of the zirconia electrode at 1273 K.

The temperature in the melt and in the gas close to the zirconia electrode was measured by means of Pt–Pt 10% Rh thermocouples (7).

### 2.2. *Chemicals and preparation of the melts*

Analytical grade anhydrous sodium tetraborate (Merck > 98%) was used as solvent. Sodium antimonate, $NaSbO_3$, the source of antimony, was obtained by dehydrating $NaSb(OH)_6$ (analytical grade, "Métallurgie Hoboken Overpelt") at 1073 K for 36 h; the dehydration reaction was controlled by thermogravimetric analysis. Potassium dichromate (analytical grade) was obtained from Merck. All the gases used were of a purity higher than 99.998% and were provided by Air Liquide.

Melts were prepared under atmospheric pressure without taking any special precautions concerning the gas phase. 100 to 200 g of $Na_2B_4O_7$ was introduced into a platinum crucible located in the heated furnace. Melting occurred rapidly, and the prepared solvent was maintained for about 10 h at high temperature. After withdrawing the crucible from the furnace, the solute was directly introduced into the liquid borate to reach a concentration of about $10^{-2}$ M.

In experiments where the melt was in equilibrium with air, the crucible was immediately replaced in the furnace; in other cases the cooled sample was introduced into the alumina cell. The temperature was gradually raised, and the gas stream was adjusted to provide the desired oxygen pressure.

Analytical determinations were carried out after equilibrium had been achieved between the melt and the gaseous atmosphere. This generally took four days as monitored by voltammetry (see below).

Some white material was distilled from the melt and was identified by X-ray diffraction as $NaBO_2$. The mean loss amount to (i) 0.77 g $NaBO_2$ per day per mole $Na_2B_4O_7$ at 1273 K under vigorous gas flow, and to (ii) 0.30 g and 0.11 g at 1273 K and 1173 K, respectively, in the absence of gas flow.

These $NaBO_2$ losses involve loss of $Na_2O$ content (according to the above conditions 0.065, 0.026 and 0.009 mol % per day). The corresponding increase in acidity was, however, negligible since sodium tetraborate is a good acidity buffer [7]. In order to prevent

significant changes, a new melt was prepared for each run involving a new $P_{O_2}$ value.

Losses of antimony have been reported in the case of silicate matrices [8] although they have not been observed during the present study.

### 2.3. *Electrochemical measurements*

The two electrode cell shown in Fig. 1 was used in all cases. The working electrodes were bright platinum foils (8) of about 0.6 $cm^2$; their areas were carefully determined by chronopotentiometric measurements in aqueous solutions of potassium hexacyanoferrate (III). The value of the diffusion constant of $Fe(CN)_6^{3-}$ as measured by Von Stackelberg *et al.* [9] has been used throughout the calculations. The crucible acted as a counter electrode.

Voltammetric measurements were carried out with a Tacussel PRG5 polarograph (9). The apparatus used for the chronopotentiometric determinations has been described previously [10]. The zirconia sensor was connected to a Tacussel ARIES 10 000 millivoltmeter (10).

## 3. Analytical procedure

### 3.1. *Results*

Figure 3 shows linear sweep voltammograms of solutions of Cr(VI)–Cr(III) and of Sb(V)–Sb(III) systems in molten sodium tetraborate, at 1273 K and under a reduced partial pressure of oxygen. In both cases, two distinct electrochemical signals were observed.

Figure 4 shows a normal pulse voltammogram of a $Na_2B_4O_7$ melt containing Sb(V) and Sb(III) under a partial pressure of oxygen of $1.69 \times 10^{-2}$ atm. At higher pressure, the reduction of dissolved oxygen in the total current has a significant influence; a blank voltammogram (dotted line) obtained for a pure borate melt was used as corrected base line.

Figure 5 shows linear cathodic sweep voltammograms of (i) a borate melt containing Cr(VI) and Cr(III) as solutes and (ii) a pure borate melt (dotted line). The partial pressure of oxygen in equilibrium with both melts was $1.36 \times 10^{-3}$ atm. The corrected voltammogram obtained by subtracting (ii) from (i) is also shown.

Differential pulse voltammograms of these melts are shown in Fig. 6.

In Table 1, the value of the peak current density measured for a total concentration of chromium of $4.5 \times 10^{-3}$ M, is presented as a function of $P_{O_2}$.

### 3.2. *Discussion*

*3.2.1. Linear sweep voltammograms.* The first waves of the voltammograms shown in Fig. 3 (at about 0 V) are mixed waves indicating that the oxidized and reduced species of reversible systems occur simultaneously in the solution. The current density of the anodic part of

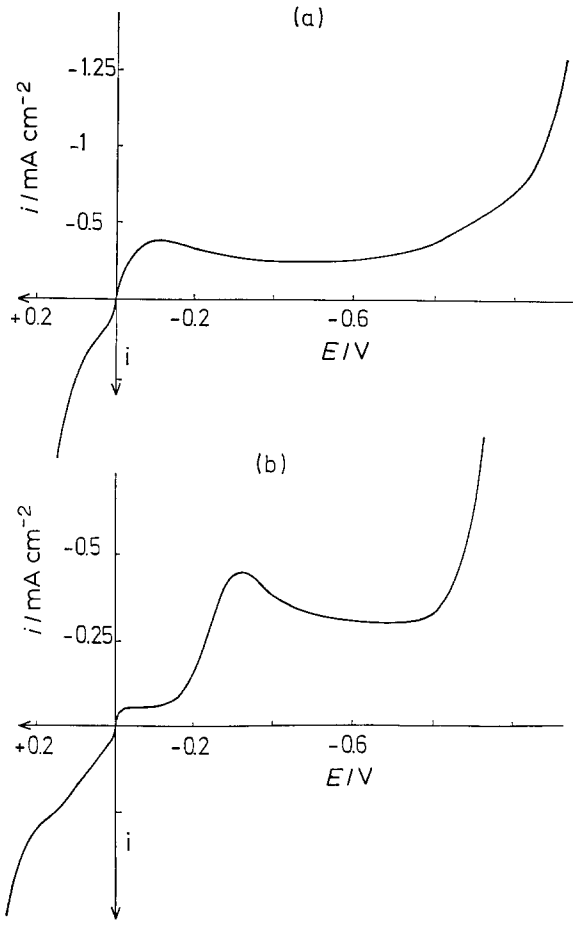


Fig. 3. Linear sweep voltammograms of $Na_2B_4O_7$ melts containing (a) the Cr(VI)/Cr(III) and (b) the Sb(V)/Sb(III) systems. Conditions: temp. 1273 K, sweep rate 10 mV $s^{-1}$ and (a) $P_{O_2} = 2.1 \times 10^{-2}$ atm, $C(Cr_{tot}) = 6.7 \times 10^{-3}$ M; (b) pure $N_2$, $C(Sb_{tot}) = 5.7 \times 10^{-3}$ M.

the mixed wave is in proportion to the concentration of the reduced species in the melt but cannot be accurately determined because of the proximity of the anodic limit of the electrochemical window. The situation is even worse in the case of oxygen partial pressures higher than $10^{-2}$ atm. However, the cathodic currents of the mixed waves are in proportion to the concentrations of the oxidized states and are readily measurable.

The second waves correspond to the reduction to the elemental state of the solute from its oxidized or

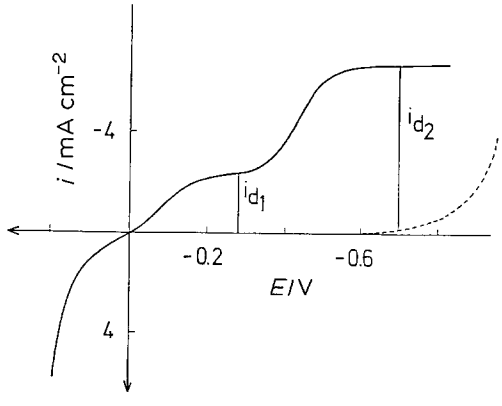


Fig. 4. Normal pulse voltammogram of $Na_2B_4O_7$ melts containing Sb(V) and Sb(III) under $P_{O_2}$ of $1.69 \times 10^{-2}$ atm and at 1273 K.

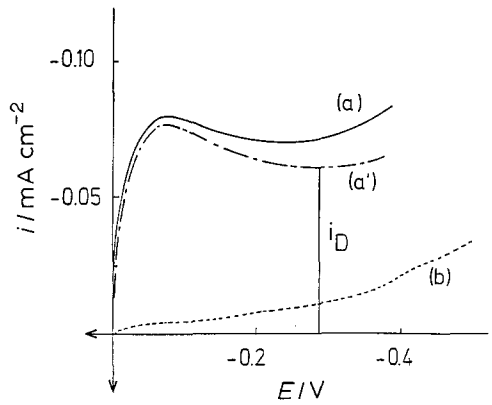


Fig. 5. Linear sweep voltammograms (a) of a solution of the Cr(VI)/Cr(III) system in molten borate and (b) of the pure borate solvent. The corrected voltammogram (a') is obtained by substracting (b) from (a) ($v = 4\,mV\,s^{-1}$).

from its reduced forms. For both systems, the second and first waves are clearly separated. Unfortunately, the current density of the Cr(III)–Cr(0) wave cannot be measured accurately because the wave spreads out over the cathodic limit of the solvent; in the case of the antimony system, however the second wave is distinct from the solvent limit. The determination of the ratio of the concentrations of the oxidized to the reduced species ($R$) is thus easier in the case of antimony and different analytical procedures were used for the two systems.

Furthermore, oxygen dissolved in the melt is reduced to oxide ions at potentials ranging from the rest potential to the cathodic limit of the electrochemical window. The corresponding amount has to be subtracted from the electrochemical signals arising from the other solutes.

*3.2.2. Analytical procedure for the antimony system.* Most electroactive species are dissolved in molten borates as oxyanions with coordination numbers depending on their oxidation state and their decomposition potentials are dependent on the activity of oxide

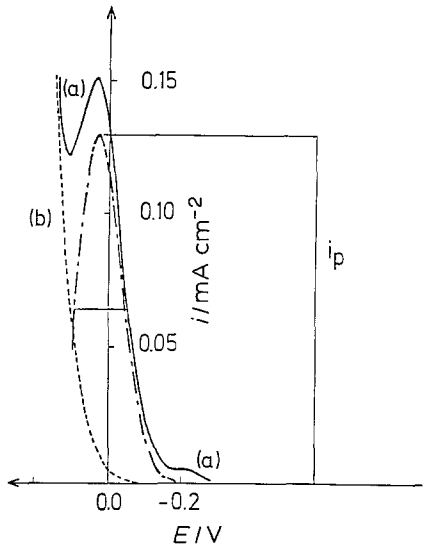


Fig. 6. Differential pulse voltammograms (a) of a solution of the Cr(VI)/Cr(III) system in molten borate and (b) of the pure borate solvent ($v = 4\,mV\,s^{-1}$).

*Table 1. Influence of $P_{O_2}$ on the peak current density of the differential pulse voltammogram of the Cr(VI)/Cr(III) system*

| $(P_{O_2})$ cell (*atm*) | $i_p$ ($mA\,cm^{-3}$) |
|---|---|
| 0.209 | 0.135 |
| $1.36 \times 10^{-2}$ | 0.130 |
| $1.36 \times 10^{-3}$ | 0.128 |
| $2.54 \times 10^{-4}$ | 0.139 |

ions in the melt. However, the oxide ion activity in the melt close to the electrode might be modified during an electrochemical reaction by an oxide ion release or consumption which would be due to the reaction itself, or by the reduction of dissolved oxygen. It is thus useful to limit the total charge exchange during the electrochemical determination and for this, normal pulse voltammetry has been selected.

The ratio of the concentrations of Sb(V) to Sb(III) is obtained from the values of the limiting currents of the first and second waves ($i_{d1}$ and $i_{d2}$) of normal pulse voltammograms (Fig. 4). These currents are described by the following equations [11]:

$$i_{d1} = 2k[\mathrm{Sb(V)}]D^{1/2}_{\mathrm{Sb(V)}} \quad (3)$$

$$i_{d2} = 5k[\mathrm{Sb(V)}]D^{1/2}_{\mathrm{Sb(V)}} + 3k[\mathrm{Sb(III)}]D^{1/2}_{\mathrm{Sb(III)}} \quad (4)$$

where $k$ is a constant which depends on the length of the pulse. The ratio $R$, easily obtained from [3] and [4], is given by

$$R = \frac{[\mathrm{Sb(V)}]}{[\mathrm{Sb(III)}]} = \frac{1}{R_D}\left(\frac{1.5i_{d1}}{i_{d2} - 2.5i_{d1}}\right) \quad (5)$$

$R_D$ is the square root of the ratio of the diffusion constants of the solutes and is expressed as $R_D = (D_{\mathrm{Sb(V)}}/D_{\mathrm{Sb(III)}})^{1/2}$. Since accurate data about diffusion constants of solutes in molten borates are not available in the literature, a $R_D$ value of 1 has been assumed. Any deviation from this value would affect all the $R$ values with an identical systematic error.

*3.2.3. Analytical procedure for the chromium system.* As the second wave of normal pulse voltammograms of melts containing chromium lies too close to the cathodic limit, linear sweep voltammograms and differential pulse voltammograms are preferably applied in order to determine the ratio of the concentrations of Cr(VI) and Cr(III).

The corrected limiting current density ($i_d$), measured under stationary diffusion conditions (Fig. 5) is in proportion to the concentration of Cr(VI) according to Equation 6:

$$i_d = k_1[\mathrm{Cr(VI)}]D^{1/2}_{\mathrm{Cr(VI)}} \quad (6)$$

The corrected peak current density of a differential pulse voltammogram (Fig. 6) depends on the concentrations of Cr(VI) and Cr(III) in the melt:

$$i_p = k_2([\mathrm{Cr(VI)}]D^{1/2}_{\mathrm{Cr(VI)}} + [\mathrm{Cr(III)}]D^{1/2}_{\mathrm{Cr(III)}}) \quad (7)$$

The proportionality constants $k_1$ and $k_2$ both depend on the temperature; $k_2$ also depends on the amplitude and length of the pulse.

If, as in the case of the antimony system, it is assumed that the diffusion constants of the oxidized and reduced species are equal, the following equation may be deduced from Equations 6 and 7:

$$R = \frac{[\text{Cr(VI)}]}{[\text{Cr(III)}]} = \frac{i_d}{k_3(I_p - i_d)} \qquad (8)$$

where $k_3$ is $k_1/k_2$.

Equation 7 shows that, if the assumption concerning the equality of the diffusion constants is correct, the peak current density measured for a given total chromium concentration does not depend on the partial pressure of oxygen in equilibrium with the melt. From Table I it appears that $i_p$ does not depend on $P_{O_2}$, and this agrees with the assumption concerning the diffusion constants of Cr(V) and Cr(III).

A comparison of Equations 5 and 8 indicates an important difference between the Sb and Cr systems: whereas the $R$ value is straightforwardly deduced from the experimental results in the case of antimony, in the case of chromium it is necessary to know the constant $k_3$. This constant has been calculated from Equation 8 using the experimental values $i_p$ and $i_d$ for a melt in equilibrium with the atmospheric pressure ($P_{O_2}$ = 0.209 atm) and an $R$ value which has been chemically determined by Gangopadhyay [12]. The $k_3$ value thus calculated is 0.604 at 1273 K.

The results obtained for the chromium system are thus dependent on a calibration procedure involving the chemical analysis of one quenched sample in the series whereas the results for the antimony system need no other data to calculate the redox ratio.

The [Cr(VI)]/[Cr(III)] ratio in molten $Na_2O$–$B_2O_3$ mixtures of various compositions equilibrated with air at 1273 K has recently been determined by Lee and Brückner using spectrophotometric and ESR measurements on annealed samples [13, 14]. An $R$ value of 0.68 has been evaluated by linear interpolation of their results for a composition corresponding to molten tetraborate. This ratio is quite different from the value of 3.55 advanced by Gangopahyay [12]. We have selected this value because the author clearly demonstrates the achievement of equilibrium conditions in his experiments. $Cr_2O_3$ and $K_2Cr_2O_7$ were used as solutes in two different samples and the melts were allowed to remain in contact with air until the same $R$ ratios were determined in both cases.

## 4. Interaction between the oxygen-oxide system and multivalent solutes

### 4.1. *Results*

*4.1.1. Electrochemical behaviour of dissolved oxygen.* Figure 7 shows a linear sweep voltammogram of oxygen dissolved in a pure borate melt. The influence of the potential scan rate on the peak potential and the peak current density has been investigated. The results are shown in Table 2.

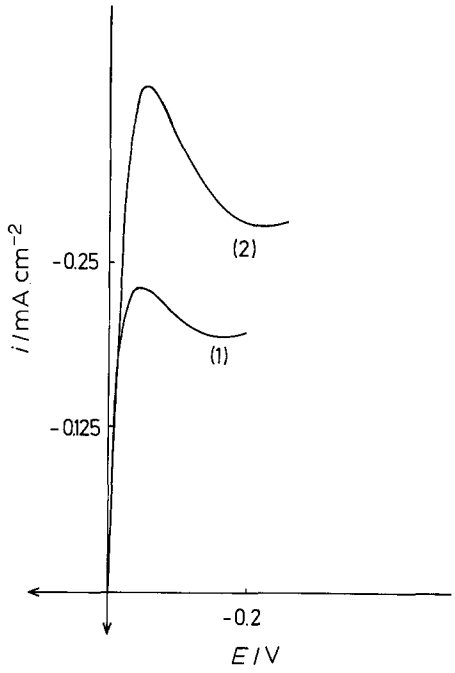


Fig. 7. Linear sweep voltammograms of a solution of oxygen in a pure borate melt: (1) 40 mV s$^{-1}$; (2) 100 mV s$^{-1}$; $P_{O_2}$ = 0.209 atm.

The dependence of the peak current density on the square root of the scan rate is shown in Fig. 8.

The potential of a platinum electrode placed near the surface of the melt was measured at various $P_{O_2}$ against the peak potential (linear sweep voltammetry) of the Sb(III)/Sb(0) system which has been shown to exhibit reversible behaviour. The potential of the platinum electrode is plotted against ln $P_{O_2}$ in Fig. 9.

*4.1.2. R values.* The ratio of the concentration of the oxidized species to that of the reduced species ($R$) has been measured at 1273 K for the Cr(VI)–Cr(III) and Sb(V)–Sb(III) systems in borate melts, when equilibrated with partial pressures of oxygen extending respectively from $2 \times 10^{-2}$ atm to 0.76 atm and from $5 \times 10^{-5}$ atm to 0.105 atm. The $R$ values are given as a function of $P_{O_2}$ (atm) in Table 3. Log $R$ is plotted against log $P_{O_2}$ in Fig. 10 for the two systems investigated.

### 4.2. *Discussion*

*4.2.1. Electrochemical behaviour of dissolved oxygen.* The irreversible electrochemical behaviour of the

*Table 2. Linear sweep voltammetry of dissolved oxygen: dependence of the peak potential and of the peak current density on the scan rate*

| $v$ ($mV s^{-1}$) | $E_p$ ($V$) | $i_p$ ($mA cm^{-2}$) |
|---|---|---|
| 10 | −0.050 | 0.118 |
| 20 | −0.050 | 0.166 |
| 40 | −0.050 | 0.238 |
| 100 | −0.055 | 0.396 |
| 200 | −0.080 | 0.569 |
| 400 | −0.125 | 0.790 |

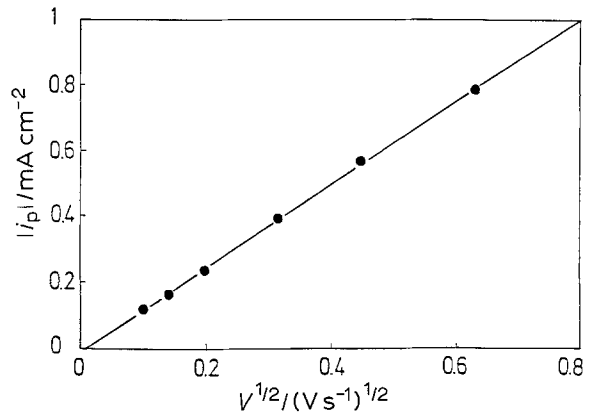


Fig. 8. Linear sweep voltammetry of dissolved $O_2$: $i_p$ against $v^{1/2}$ with air at 1273 K.

*Table 3. Influence of the partial pressure of oxygen on the ratio R for the chromium (VI–III) and antimony (V–III) redox systems*

| $P_{O_2}$ (atm) | $\frac{Cr(VI)}{Cr(III)}$ | $\frac{Sb(V)}{Sb(III)}$ |
|---|---|---|
| $5.0 \times 10^{-5}$ | – | 0.105 |
| $2.5 \times 10^{-4}$ | – | 0.225 |
| $1.7 \times 10^{-2}$ | – | 3.55 |
| $2.1 \times 10^{-2}$ | 0.76 | – |
| $2.7 \times 10^{-2}$ | 0.82 | – |
| $8.0 \times 10^{-2}$ | – | 5.18 |
| 0.105 | 1.46 | 6.12 |
| 0.209 | 3.55 | – |
| 0.76 | 9.0 | – |

$O_2/O(-II)$ redox system in solutions at room temperature is well known. As the reaction rate increases with temperature, Nernstian behaviour is reached when the temperature is sufficiently high.

The linear dependence of the peak current density on the square root of the potential scan rate (Fig. 8) shows that transport occurs according to a linear semi-infinite diffusion model, and that the redox system is either Nernstian or totally irreversible [15].

The independence of the peak potential on the sweep rate over a range extending from 10 mV s$^{-1}$ to 100 mV s$^{-1}$ (Table 2) indicates that the redox system of oxygen behaves reversibly at sweep rates lower than 100 mV s$^{-1}$. The slope of the diagram that describes the dependence of the potential of a platinum electrode on the partial pressure of oxygen (Fig. 9) amounts to 0.025 V per logarithmic unit compared to the theoretical slope of 0.027 V per logarithmic unit calculated from the Nernst equation for the ($O_2 + 4e^- \rightarrow 2O^{2-}$) redox system at 1273 K. This excellent agreement corroborates the reversible behaviour of the oxygen system at 1273 K.

*4.2.2. R values.* An increase of the *R* ratio with oxygen pressure has often been found in the chemical analysis of quenched samples [5, 16–19]. An increase of the basicity of the melt has been shown to stabilize the highest oxidation states of multivalent elements in oxide melts whereas the redox potential of the *in situ* systems decreases at the same time [8, 20–24]. This may be explained if the complexing properties of oxide ions are taken into account, since the number of oxide ions coordinated to a cation of a given element very often increases with the oxidation state.

The redox equilibrium involving the oxygen system and the $M^{(m+n)+}/M^{m+}$ system may be written:

$$4MO_x^{(2x-m)-} + nO_2 + 2(2y - 2x - n)O^{2-} \rightleftharpoons 4MO_y^{(2y-m-n)-} \quad (9)$$

The symbols $y$ and $x$ are the coordinators of $M^{(m+n)+}$ and $M^{m+}$, respectively. An increase in basicity stabilizes the highest oxidation state if the stoichiometric coefficient of $O^{2-}$ in Equation 9 is positive, that is, if

$$y - x > n/2 \quad (10)$$

The equilibrium constant of Equation 9 is

$$K = \frac{(a_{MO_y}^{(2y-m-n)-})^4}{(a_{MO_x}^{(2x-m)-})^4 f_{O_2}^n a_{O^{2-}}^{(4y-4x-2n)}} \quad (11)$$

where $f_{O_2}$ is the fugacity of oxygen and $a_i$ the activity of species $i$. Rewriting Equation 11 in a logarithmic form leads to

$$4 \ln R_a = \ln K + n \ln f_{O_2} + (4y + 4x - 2n) \ln a_{O^{2-}} \quad (12)$$

$R_a$ being the ratio of the activities of the oxidized and reduced species.

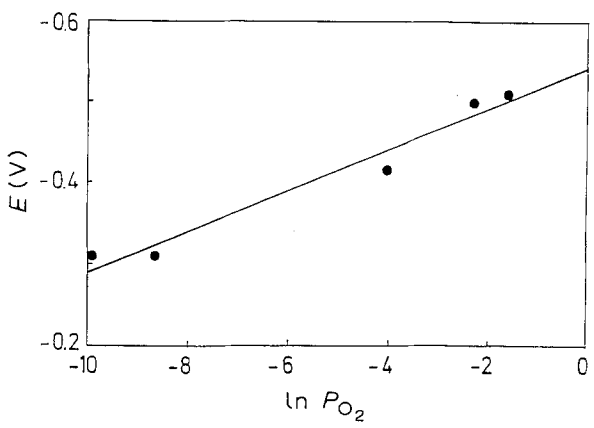


Fig. 9. $P_{O_2}$ dependence of the potential of a platinum electrode.

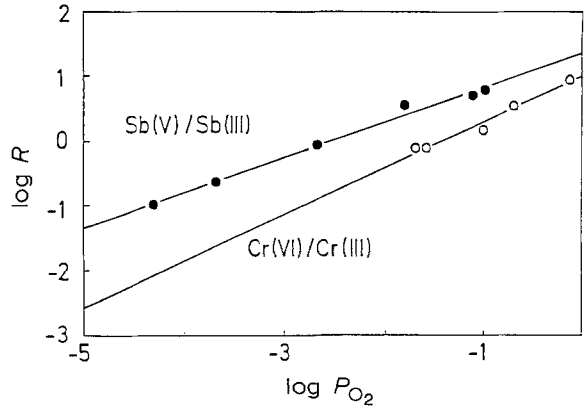


Fig. 10. Influence of the partial pressure of oxygen on the redox ratios [Sb(V)]/[Sb(III)] and [Cr(VI)]/[Cr(III)] at 1273 K.

Introducing the activity coefficients ($\gamma$), gives

$$\ln R = \tfrac{1}{4}\ln K - \ln \frac{\gamma(MO_y^{(2y-m-n)-})}{\gamma(MO_x^{(2x-m)-})} + \frac{n}{4}\ln P_{O_2} + \frac{n}{4}\ln \gamma_{O_2} + \left(y - x - \frac{n}{2}\right)\ln a_{O^{2-}} \quad (13)$$

The equilibrium constant of Reaction 9 can be related to the difference in the standard potentials of the interacting systems according to

$$\ln K = -\frac{\Delta G^\circ}{RT} = \frac{4nF\Delta E^\circ}{RT} = \frac{4nF}{RT}[E^\circ(O_2) - E^\circ(M)] \quad (14)$$

where $E^\circ(O_2)$ and $E^\circ(M)$ are the standard potentials of the following systems:

$$O_2 + 4e^- \rightleftharpoons 2O^{2-}$$

and

$$MO_y^{(2y-m-n)-} + ne^- \rightleftharpoons MO_x^{(2x-m)-} + (y - x)O^{2-}$$

According to the concentration units used in this work, the reference state for the solutes is infinite dilution in a melt having the properties of a pure melt. The standard state corresponds to a 1 M concentration of the solutes in their reference state; this standard state is thus a fictitious one and the definition is not very apposite to the oxide ion since the oxide ion activity may not be changed without modifying the matrix. It may, however, be adopted if the composition of the melt remains constant. The standard state of oxygen is the pure gas at a pressure of 1 atmosphere and should follow an ideal gas behaviour.

Rearrangement of Equations 13 and 14 yields

$$\ln R = \frac{n}{4}\ln P_{O_2} + \frac{nF}{RT}\left\{\left[E^\circ(O_2) + \frac{RT}{4F}\ln \gamma_{O_2} - \frac{RT}{2F}\ln a_{O^{2-}}\right] - \left[E^\circ(M) + \frac{RT}{nF}\ln \times \frac{\gamma(MO_y^{(2y-m-n)-})}{\gamma(MO_x^{(2x-m)-})} + \frac{RT}{nF}(x - y)\ln a_{O^{2-}}\right]\right\} \quad (15)$$

The first series of bracketed terms is the potential of an oxygen electrode when the investigated melt is in equilibrium with oxygen at a partial pressure of 1 atm ($E^{\circ\prime}(O_2)$). The second series of bracketed terms is the potential of the $(MO_y^{(2y-m-n)-})/(MO_x^{(2x-m)-})$ system for unit concentrations of the reduced and oxidized species, i.e. the formal potential ($E^{\circ\prime}(M)$) of the solute redox system for the oxide ion activity of the pure melt.

Hence, Equation 15 becomes

$$\ln R = \frac{n}{4}\ln P_{O_2} + \frac{nF}{RT}[E^{\circ\prime}(O_2) - E^{\circ\prime}(M)]$$

or

$$\log R = \frac{n}{4}\log P_{O_2} + \frac{nF}{2.303RT}[E^{\circ\prime}(O_2) - E^{\circ\prime}(M)] \quad (16)$$

The difference $[E^{\circ\prime}(O_2) - E^{\circ\prime}(M)]$ is the formal potential of the solute system as referred to a 1 atm oxygen electrode.

According to Equation 16, the slopes of the straight lines in Fig. 11 should be in parallel with the number of electrons exchanged by the investigated redox systems. The experimental values of the slopes, 0.72 for Cr(VI)/Cr(III) and 0.54 for Sb(V)/Sb(III) are in excellent agreement with the theoretical values characteristic for equilibrium conditions (Equation 16), i.e. respectively 3/4 and 2/4. Similar results are described in the literature [4, 25], but contrary to the data, the present results are derived from analyses which have been carried out in the melt at 1273 K and are therefore free from any approximations which may be involved when the analyses are carried out on quenched samples. This is particularly true for the investigation of the antimony system which is based exclusively on measurements performed on the liquid phase. In the case of the chromium system, the analytical procedure has been calibrated with regard to the $R$ value determined by chemical analyses of quenched samples of a borate melt previously equilibrated with air. This method might introduce a systematic error in the $R$ values but the slope of the experimental straight line would not be affected in this situation.

In Fig. 11, the ordinates at zero abscissa for the antimony and chromium systems are respectively 1.36 and 1.02 decimal logarithmic units. According to Equation 16, if a value of 0 V is assigned to the 1 atm oxygen elecrode, then

$$E^{\circ\prime}(Sb(V)/Sb(III)) = \frac{1.36 \times 0.252}{2} = -0.17\,V$$

and

$$E^{\circ\prime}(Cr(VI)/Cr(III)) = \frac{1.02 \times 0.252}{3} = -0.09\,V$$

## 5. Conclusions

An *in situ* voltammetric determination of the redox ratios [Sb(V)]/[Sb(III)] and [Cr(VI)]/[Cr(III)] in molten tetraborate has been carried out. Contrary to previously described procedures, which are based on potential measurements [2, 6], the redox ratios were evaluated from current determinations which offer at least two major advantages:

(i) they are more accurate than potential determinations when the concentration of the oxidized and reduced species are close together, and

(ii) they may be used even when the investigated redox system exhibit a non Nernstian behaviour.

The reversible behaviour of the oxygen-oxide redox system in molten tetraborate has been confirmed from voltammetric and potentiometric determinations.

Finally, the developed analytical procedure has been used to verify the achievement of a state of equilibrium in melts containing oxygen and multivalent solutes and the influence of the partial pressure

of oxygen upon the redox ratios of antimony and chromium was investigated. The experimental results are in excellent agreement with the theoretical relationship characteristic of equilibrium conditions. This result was reached earlier from chemical and instrumental analysis of quenched samples of melts previously equilibrated with gaseous atmosphere containing adjusted partial pressures of oxygen. To our knowledge, these results are the first experimental demonstration of the determination of the redox properties by the oxygen partial pressure in borate melts from *in situ* high temperature measurements.

## Acknowledgements

This research received financial assistance from the F.R.F.C. (Fonds de la Recherche Fondamentale et Collective). One of the authors is indebted to the A.G.C.D. (Administration Générale pour la Coopération au Développement) for financial support. The authors thank Professor D. Inman for language help.

## References

[1] P. Claes and J. Glibert, *Rivista della Stazione sperimentale del Vetro*, **5** (1985) 229.
[2] E. Freude and C. Rüssel, *Glastech. Ber.* **60** (1987) 202.
[3] C. Montel, C. Rüssel and E. Freude, *ibid.* **61** (1988) 59.
[4] C. Rüssel, R. Kohl and H. A. Schaeffer, *ibid.* **61** (1988) 209.
[5] W. D. Johnston, *J. Amer. Ceram. Soc.* **48** (1965) 184.
[6] K. Suzumura, K. Kawamura and T. Yokokawa, submitted to *Trans. Faraday Soc.*
[7] M. Günaltun, Ph.D. thesis, Grenoble (France) (1981).
[8] P. Nath and R. W. Douglas, *Phys. Chem. Glasses* **6** (1965) 197.
[9] M. Von Stackelberg, M. Pilgram and V. Toome, *Z. Electrochem.* **57** (1953) 342.
[10] M. Declercq and A. Withagen-Declercq, *Anal. Chim. Acta* **63** (1973) 427.
[11] A. J. Bard and L. R. Faulkner, 'Electrochemical Methods – Fundamentals and Applications', J. Wiley and Sons, New York (1980) p. 187.
[12] P. K. Gangopadhyay, *Trans. Indian Ceramic Soc.* **38** (1979) 219.
[13] J. H. Lee and R. Brückner, *Glastech. Ber.* **57** (1984) 7.
[14] *Idem, ibid.* **59** (1986) 233.
[15] A. J. Bard and L. R. Faulkner, *op. cit.* [11], p.218 and p. 222.
[16] P. Close, H. M. Sheperd and C. H. Drummond, *J. Amer. Ceram. Soc.* **41** (1958) 455.
[17] W. D. Johnston, *ibid.* **47** (1964) 198.
[18] W. Iwamoto and Y. Makino, *Transactions J. Welding Res. Inst. Japan* **8** (1979) 39.
[19] Y. Makino, S. Morita, M. Sugizaki and K. Sugaya, *Rep. Res.. Lab. Asaki Glass Co., Ltd.* **30** (1980) 59.
[20] A. Paul and R. W. Douglas, *Phys. Chem. Glasses* **6** (1965) 212.
[21] H. V. Lauer Jr. and R. V. Morris, *J. Amer. Ceram. Soc.* **60** (1977) 444.
[22] H. V. Lauer Jr., *Phys. Chem. Glasses* **18** (1977) 49.
[23] R. Pyare, S. P. Singh, A. Singh and P. Nath, *ibid.* **23** (1982) 158.
[24] R. Pyare and P. Nath, *J. Amer. Soc.* **65** (1982) 550.
[25] H. D. Schreiber, *J. Non-Cryst. Solids* **42** (1980) 175.